Original Article

Amir Ghavidel, Amin Jorbandian, Miklós Bak, Jana Gelbrich, Jeffrey J. Morrell, Ion Sandu and Reza Hosseinpourpia*

Degradation assessment of archaeological oak (*Quercus* spp.) buried under oxygen-limited condition

https://doi.org/10.1515/hf-2022-0168
Received November 1, 2022; accepted December 16, 2022; published online January 4, 2023

Abstract: The biological deterioration of archaeological wood under oxygen-limited conditions varies due to the limited activities of microorganisms. It is essential to expand the knowledge of the degradation types and the status of archaeological monuments for selecting the proper consolidates. The physical, chemical, and anatomical properties of approximately 600–650 year old archaeological oak collected from an archaeological site in Iasi-Romania were analysed to assess the quality and to identify the degradation types. The results were compared with similar tests on recently-cut oak. X-ray photoelectron spectroscopy (XPS) revealed the presence of more lignin-related peaks in the archaeological oak, which likely reflected the degradation of the wood carbohydrates as evidenced by the decreased oxygen-to-carbon ratio $C_{ox}/C_{non\text{-}ox}$. The differences in cellulose crystallinity were not significant suggesting that any cellulose degradation occurred in the amorphous regions. This was also reflected in the dynamic water vapor sorption analysis where the differences in sorption isotherms and hysteresis of archaeological and recently-cut oaks were marginal. Microscopic analysis of the oak cells illustrated bacterial degradation patterns, while the field emission scanning electron microscopy (FESEM) showed the presence of erosion bacteria in the archaeological oak collected from the site with low oxygen conditions.

Keywords: archaeological wood; AVS; biological degradation; erosion bacteria; XPS.

***Corresponding author: Reza Hosseinpourpia**, Department of Forestry and Wood Technology, Linnaeus University, Lückligs Plats 1, 351 95 Växjö, Sweden; and College of Forest Resources and Environmental Science, Michigan Technological University, Houghton, MI 49931, USA, E-mail: reza.hosseinpourpia@lnu.se. https://orcid.org/0000-0003-0883-2306

Amir Ghavidel, Department of Forestry and Wood Technology, Linnaeus University, Lückligs Plats 1, 351 95 Växjö, Sweden. https://orcid.org/0000-0002-1220-0443

Amin Jorbandian, Department of Wood and Paper Science and Technology, University of Tehran, Tehran, Iran

Miklós Bak, Institute of Wood Technology and Technical Sciences, University of Sopron, Sopron, Hungary. https://orcid.org/0000-0003-4378-7838

Jana Gelbrich, Leibniz-IWT – Institute for Materials Testing, Paul-Feller Strasse 1, 28199 Bremen, Germany

Jeffrey J. Morrell, Centre for Timber Durability and Design Life, University of the Sunshine Coast, 41 Boggo Road, Dutton Park, QLD 4102, Australia

Ion Sandu, Academy of Romanian Scientists (AOSR), 54 Splaiul Independentei St., Sect. 5, 050094 Bucharest, Romania; and Romanian Inventors Forum, Iasi, 3 Sf. Petru Movila Street, Bloc L11, Sc. A, Et. 3, Ap. 3, 700089 Iasi, Romania. https://orcid.org/0000-0003-4088-8967

1 Introduction

The use of wood has evolved over time from a simple, readily available natural material to a modern engineered, smart material with unique attributes (Ghavidel et al. 2021a, 2021b; Walsh-Korb and Avérous 2019). While among the most durable cellulosic materials, wood can be biologically degraded under the proper environmental conditions. These conditions typically involve moisture levels above the fiber saturation point coupled with adequate oxygen and suitable temperatures. Fungi and insects are the primary agents of deterioration under these conditions, and can rapidly degrade wood in a variety of environments.

However, there is an entirely different pathway for deterioration when the wood is buried in wet soils or submerged in fresh water for long periods. Oxygen is typically limited under these conditions, excluding most fungi and insects. Bacteria, especially anaerobic bacteria, become the dominant agents of degradation under these conditions. The buried or submerged wood becomes waterlogged, limiting oxygen availability. Degradation proceeds from the outer surface inward, creating a distinct band of heavily degraded and softened wood on the surface surrounding a relatively sound core. This pattern is often observed in oak owing to the combination of density and the presence of extractives

(Bjurhager et al. 2012). Wood-degrading bacteria have developed mechanisms for degrading the lignocellulosic matrix, such as resistance to wood preservatives and heartwood extractives as well as the ability to function at extremely low oxygen levels (Gelbrich 2009). Bacteria degradation patterns can easily be distinguished from those produced by fungi because the micromorphological patterns created in the wood cell walls are distinctive and quite different from fungal decay patterns (Feist 1989; Florian 1989; Kránitz et al. 2016). Erosion and tunneling are two unique types of bacterial degradation (Björdal et al. 2000; Gelbrich et al. 2008), with erosion becoming more common in buried archaeological wood (Ghavidel et al. 2021b; Lucejko et al. 2020).

Hemicellulose is the first of the cell wall polymers to be degraded under anaerobic conditions, followed by cellulose (Björdal et al. 2000; Ghavidel et al. 2020a, 2022). Lignin is most resistant to bacterial degradation. As a result, the proportion of lignin in archaeological woods is higher than in recently-cut wood (Baar et al. 2020; Gelbrich 2009). The resulting shifts in hemicellulose, cellulose, and lignin ratios affect sorption behavior, mechanical strength, physical and morphological properties (Björdal et al. 2000; Esteban et al. 2009). Moisture sorption behavior of archaeological wood has been inconsistent. Popescu and Hill (2013) found that preferential degradation of wood polysaccharides left large amounts of lignin that were associated with lower moisture sorption in historical *Tilia cordata* wood compared to recently cut timber of the same species. Archaeological *Pinus yunnanensis;* however, has higher moisture levels and experiences greater longitudinal shrinkage as compared with the control samples due to the decomposition of the polysaccharides and reduced cellulose crystallinity (Jingran et al. 2014). Similar results were reported elsewhere (Baar et al. 2020; Esteban et al. 2009; Ghavidel et al. 2020b, 2020c). The archaeological wood samples in these studies were primarily exposed under oxygen-rich conditions that would allow for periodic aerobic degradation.

Degradation mechanisms under oxygen-limited conditions still involve cellulose and hemicellulose hydrolysis, but since the majority of microbial lignolytic enzymes require the presence of oxygen, aerobic conditions are essentially the only ones where total lignin degradation may occur, while anaerobic conditions impose slow lignin degradation (Dao et al. 2018; Gelbrich 2009; Unger et al. 2001). However, it should be noted that some lignin degradation can occur under low oxygen conditions. For example, moderately decayed archaeological *Hopea* and *Tectona* from the Xiaobaijiao shipwreck had higher moisture contents in comparison with less decayed samples due to the lower amounts of cellulose and hemicellulose and the proportionally higher amounts of lignin (Han et al. 2020). Esteban et al. (2009) reported higher moisture sorption and hysteresis coefficients in 1170 (±40) BP year old juvenile *Pinus sylvestris* L. wood from a site in San Martin de la Vega del Alberche, in Avila (Spain) under low oxygen conditions. Ghavidel et al. (2020a) found decreased cellulose crystallinity due to bacterial degradation of elm and poplar archaeological wood samples.

Characterising the degradation patterns in archaeological timbers can have important implications for developing effective conservation and restoration strategies. Rising interest in preserving evidence of ancient cultures has resulted in an increasing number of excavations as well as the recovery of artifacts in various stages of degradation. For example, ~600 to 650 year-old oak (*Quercus* spp) timbers were recently discovered in Isai City, Romania. The timbers had been exposed under low oxygen conditions and contained evidence of biological degradation. Understanding the degree of decomposition in relation to the residual chemical and physical properties is an important aspect of identifying effective restoration strategies. The primary objective of this study was to characterise the properties of these archaeological timbers as part of the restoration process.

2 Materials and methods

2.1 Sample preparation

The archaeological oak samples were 1 m long beams presumed to be from a fence from an 14th-century archaeological site called Olita Mate located on Armenia Street in Iasi city, Romania. The archaeological oak wood beams were used for paving and arranged vertically embedded in the clay soil of the central street and covered with macadam paving (cubic stone with dimensions of approx. 150 × 150 × 150 mm) of granite and diorite. The stone pavement was eventually destroyed, and the archaeological oak beam samples were buried to a depth of approximately 2 m. 250 archaeological beams were extracted on site and 6 of them were brought to the ARHEOINVEST laboratory (Iasi, Romania) for dendrochronological analysis and degradation assessment. Despite the sample age, the wood structure was intact but darkly discoloured by the presence of iron that had reacted with the tannins to form iron tannate (Figure 1), as described previously (Ghavidel et al. 2020d). The beams

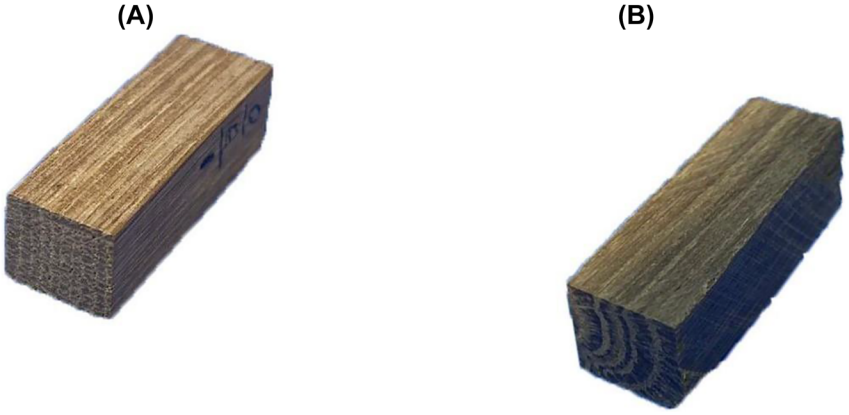

Figure 1: Recently-cut (A) and archaeological oak (B).

were in the form of trunks with a diameter of less than 300 mm, covered with tree bark. The outer 15 mm of each sample was heavily encrusted with soil and was cut away to facilitate sample preparation. Three discs were extracted from each beam, and then samples with size of $10 \times 10 \times 30$ (± 0.5) ($R \times T \times L$) mm^3 were cut from each disc. The control samples were obtained from a 45 mm by 90 mm by 4 m long defect-free board obtained from the Iasi region in Romania. Only defect-free samples (without knots, cracks, or reaction wood, and with an annual growth ring slope of less than 5°) were used for the testing. The moisture contents at the time of collection of the archaeological and recently-cut oak were 9.3 and 7.6%, respectively. The respective oven dry density of the recently-cut and archaeological oak samples were 730 kg/m^3 and 660 kg/m^3. Samples from heartwood were used for both recently-cut and archaeological wood.

2.2 X-ray photoelectron spectroscopy (XPS)

Chemical compositions of wood samples were examined at room temperature using a concentric hemispherical electron energy analyser (CHA) (Specs model EA10 plus, Bestec Co, Berlin, Germany) with an Al-Kα radiation source, a photonic energy of 1486.6 eV, and a base pressure of 2 µPa, as described previously (Ghavidel et al. 2020a, 2020b). Three samples were selected randomly from different parts of archaeological and recently-cut samples, two measurements were performed per sample, and the average value was reported (n = 6).

2.3 X-ray diffraction analysis (XRD)

The crystalline structure of the samples was measured on wood ground to pass a 10 µm mesh screen (P7 premium, Fritsch) on a Philips X'Pert MPD PW 3040 X-ray diffractometer (Netherlands) equipped with a PW 3050/10 goniometer, divergence slit 0.5°, antiscatter slit 0.5°, receiving slit 0.6 mm, secondary graphite monochromator, mask 15 mm, 40 kV activity and 30 mA with Cu Kα radiation. Analysis was carried out in a continuous mode using the scanning range of 5–50°2θ with a phase width of 0.02°2θ as previously described (Ghavidel et al. 2020a, 2020b). The sample rotating speed was 1 rpm, and each move took 4 s to count. The crystallinity index (CrI) and crystallite size were determined according to Equations (1) and (2) (Ghavidel et al. 2020b):

$$\mathrm{CrI}[\ \%\ ] = \frac{I_{200} - I_{\mathrm{am}}}{I_{200}} \times 100, \tag{1}$$

where I_{am} is the minimum intensity peaks at 2 = 16.14°, assigned to the amorphous phase, and I_{200} is the intensity of the crystalline peak at 2θ = 22.5°, allocated to both crystalline and amorphous parts.

$$L = \frac{K\lambda}{\beta \cos\theta}, \tag{2}$$

where K is a constant with the value of 0.94, λ is the X-ray wavelength, β is the full width at half maximum of the diffraction band and θ is the Bragg angle corresponding to the (200) plane.

2.4 Water sorption analysis

Water vapour sorption behavior of ground wood samples (passed through a 20 mesh sieve) was investigated using a Q5000 SA automated vapor sorption (AVS) analysis apparatus (Q5000 SA, TA Instruments) at a constant temperature of 25 °C (Ghavidel et al. 2020a; Hosseinpourpia et al. 2018, 2019, 2020). Sorption isotherm was measured from 0 to 95% relative humidity (RH) and then reversed to 0 percent RH with dm/dt criteria of less than 0.005% per 10 min. The weight at equilibrium was measured using a micro-balance at each RH, and the equilibrium moisture content (EMC) was calculated accordingly.

2.5 Microscopic analyses

The degree of damage was assessed using both light and scanning electron microscopy. Three samples from different parts of archaeological oak were selected and thin sectioned for light microscopy from the transverse and longitudinal faces of the water-soaked archaeological wood. The transverse sections were stained with 1% (w/v) safranin O in ethanol while the longitudinal sections were stained with 0.1% (w/v) aniline blue (Ghavidel et al. 2021b, 2020c). Samples were imaged with a Zeiss Axioscope equipped with AxioCam and Axio vision software (Carl Zeiss MicroImaging GmbH, Germany). The archaeological oak samples were still relatively sound and could be hand-sectioned for staining and analysis, while a large number of sections were prepared to carefully study the degradation patterns.

Recently-cut and archaeological samples were further examined using a Hitachi S-3400 N (Tokyo, Japan) scanning electron microscope

operated at an 8 kV accelerating voltage. Samples (5 mm cubes) were surfaced with a razor blade to create a smooth surface and mounted on aluminium stubs. The surfaces were examined directly without sputter coating (Ghavidel et al. 2020d, 2022). A TSCAN (Brno, Cheque Republic) FESEM was used where the higher resolution was required following a similar sample preparation method.

3 Results and discussion

3.1 Chemical structure and crystallinity of archaeological oak

X-ray photoelectron spectroscopy (XPS) analysis of the recently-cut and archaeological oak samples produced C1s energy level spectra with four sub-peaks, e.g., C1, C2, C3, and C4, and O1s energy level spectra with two sub-peaks of O1 and O2 (Figure 2).

The C1 signal (Figure 2A, B) which mainly represents the presence of extractives and lignin increased substantially in the archaeological oak with a simultaneous decrease in the concentration of oxygenated C atoms. Increasing proportions of lignin reflect the tendency for the hollocellulose components to be degraded in archaeological samples, leaving a lignin-rich residual (Capano et al. 2015; Christiernin et al. 2009). The C2 sub-peak which represent cellulose and hemicellulose was slightly lower in the archaeological oak, while the C3 and C4 sub-peaks were not markedly changed. These changes reflect the loss of low molecular weight components including extractives, hemicelluloses, and even a small portion of amorphous cellulose, which typically occurs during the first 150 years of ageing (Ghavidel et al. 2020a, 2020b; Popescu

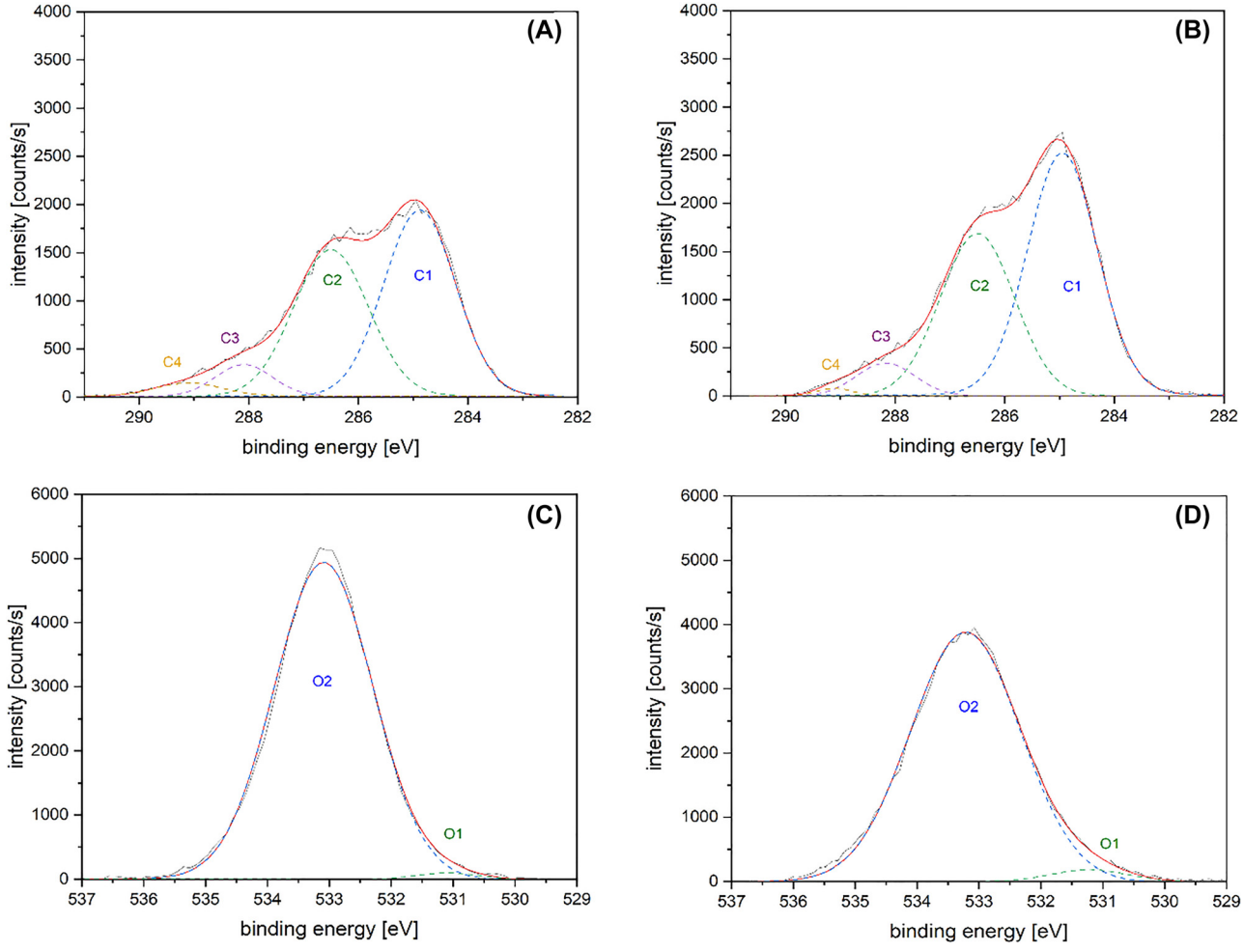

Figure 2: High–resolution spectra of the C1s and O1s energy levels of recently-cut (A, C) and archaeological samples (B, D) of oak.

et al. 2009). The higher resistance of oak to microbial attack might help explain the lower losses of these wood components. Popescu et al. (2009) reported a significant decrease in the C1 sub-peak and an increasing C2 sub-peak in archaeological lime wood as the result of an increase in C-O groups caused by oxidation and hydrolysis reactions that occurred during the ageing process. The results in the present work, however, suggest that neither oxidation nor hydrolysis occurred in the archaeological oak (Table 1). For the oxidation of lignin, oxygen is required, and the low access to oxygen in the archaeological site largely limited that process. Additionally, oxidation and hydrolysis are mutually reliant and catalyse one another. The β-glycosidic link of carbohydrates is more vulnerable to hydrolysis processes than oxidation (Łojewska et al. 2005). The oxygen/carbon ratio and C_{ox}/C_{unox} were much lower in the archaeological sample (Table 1) which could be attributed to bacterial degradation of the carbohydrates. Thus, hydrolysis may be unlikely to occur in the archaeological oak sample. The C1 sub-peak corresponding to lignin and extractives in wood was also higher in archaeological oak, supporting the premise that carbohydrates in this fraction have been preferentially degraded in archaeological oak. The decreased C_{ox}/C_{unox} also suggests an increase in C–C bonds, which tend to be more closely associated with lignin.

The O1 and O2 sub-peaks (Figure 2C, D) are related to the oxygen atoms that are linked with double and single bonds to carbon atoms, respectively (Popescu et al. 2009). The O2 sub-peak of the archaeological oak decreased, potentially as a result of hemicellulose degradation (Hedges 1989; Nzokou and Pascal Kamdem 2005; Popescu et al. 2009). Hemicellulose is considered to be the most susceptible of the three polymers to microbial degradation and can be degraded by bacteria in the absence of oxygen, while lignin degradation is oxidative and requires the presence of some oxygen (Björdal et al. 2000; Goodell et al. 2020). Oxygen is generally limited in buried substrates. These results are consistent with anaerobic bacterial degradation.

The crystalline structure and degree of crystallinity of recently-cut and archaeological oak wood samples are shown in Figure 3 and Table 2. I_{200} and I_{am} represent the maximum and minimum intensities of the crystalline cellulose, respectively. The crystalline index is shown by CrI and the crystalline size of the cellulose is represented by *L*. There were small differences in the crystallinity of cellulose between recently-cut and archaeological oak that may reflect the leaching of extractives from the archaeological materials. A small reduction in the crystalline size of the archaeological wood could be related to moisture absorption, chemical reactivity, or swelling (Lionetto et al. 2012). Although, it is known that the degradation of hemicellulose and amorphous cellulose increases the crystallinity index, the total crystallinity percentage may decrease when available degraded carbohydrates are consumed by degrading agents (Howell et al. 2009).

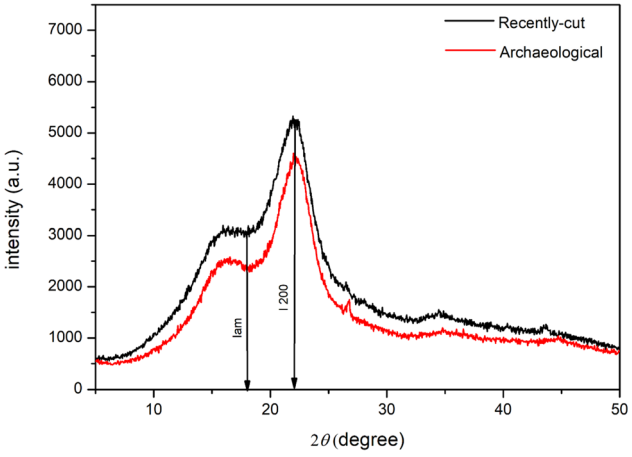

Figure 3: X-ray diffractograms from archaeological and recently-cut oak.

Table 2: Band positions of crystalline and amorphous cellulose and the calculated parameters for the wood samples.

Wood samples	*I*200	*I*am	CrI (%)	*L* (200) (nm)
Recently-cut oak	22.10	18.18	50.28	8.78
Archaeological oak	21.94	17.98	44.72	8.19

Table 1: Relative surface composition for recently-cut and archaeological oak.

Wood samples	C1 (atm.%)	C2 (atm.%)	C3 (atm.%)	C4 (atm.%)	Atomic ratio O/C	Cox/Cunox
Recently-cut oak	33.4 (±0.8)	55.21(±1.1)	7.2 (±0.9)	5.2 (±1.1)	0.44	2.02
Archaeological oak	46.7 (±3.07)	42.8 (±2.5)	6.5 (±0.8)	4.1 (±0.8)	0.32	1.14

Degradation patterns differ by deterioration agent with white rot fungi tending to erode cell walls, brown rot fungi producing a general attack that can be difficult to detect microscopically, and soft rot fungi producing either erosion of the cell wall or diamond-shaped cavities within the S_2 cell wall layer. Bacterial decay can be characterised as either erosion of the wood cell wall from the lumen outward or tunnelling within the cell wall. Bacterial decay in anoxic environments tends to start on the surface and slowly extend inwards (Björdal et al. 2000; Pedersen et al. 2021; Singh et al. 2022), degrading the wood polymers and influencing the crystalline structure of wood.

3.2 Moisture sorption of archaeological oak

Moisture sorption reflects the availability of hydroxyls on the hemicellulose and amorphous cellulose fractions of the wood and would be expected to decline as bacteria degrade this fraction (Han et al. 2020). The isotherm curves of recently cut and archaeological oak samples illustrated the typical type II sigmoid character of cellulosic materials (Figure 4). The ageing process altered the sorption behaviour of archaeological wood samples through the whole adsorption and desorption runs especially at higher relative humidities (RHs), e.g., over 80%. The archaeological oak wood reached slightly higher equilibrium moisture content (EMC) values during the sorption and desorption processes across the entire hygroscopic range. This might be attributed to the slightly lower crystallinity in the archaeological oak samples in comparison with the recently-cut one, as indicated by the XRD analysis. Figure 4B demonstrates the sorption hysteresis of oak samples. As with the sorption isotherms, the hysteresis values were similar for both sample types. These results differ from the higher EMC values found during adsorption/desorption processes with elm and poplar samples exposed for prolonged periods under low oxygen conditions (Ghavidel et al. 2020a). The differences in hysteresis may reflect variations in volumetric swelling as a result of kinetic retardation during shrinkage/swelling (Hosseinpourpia et al. 2016). The slightly higher values in sorption hysteresis of the archaeological oak might be related to reduced flexibility of wood cells and/or fewer hydroxyl groups, as a result of the degradation and ageing processes. Degradation of amorphous cellulose and hemicellulose over time might also result in a more stable and lower degradation rate of crystalline cellulose levels (Howell et al. 2009). Moreover, the degradation of hemicellulose in archaeological wood reduces the length of the crystal regions, which may result in the appearance of new absorption sites (Guo et al. 2018), and, consequently, increment of equilibrium moisture content.

3.3 Morphology of the degraded wood

The optical microscopy images were shown in Figure 5A–C. Light microscopic examination of transverse -sections of degraded cells indicated that decay started in the lumen and progressed outwards until it reached the middle lamella

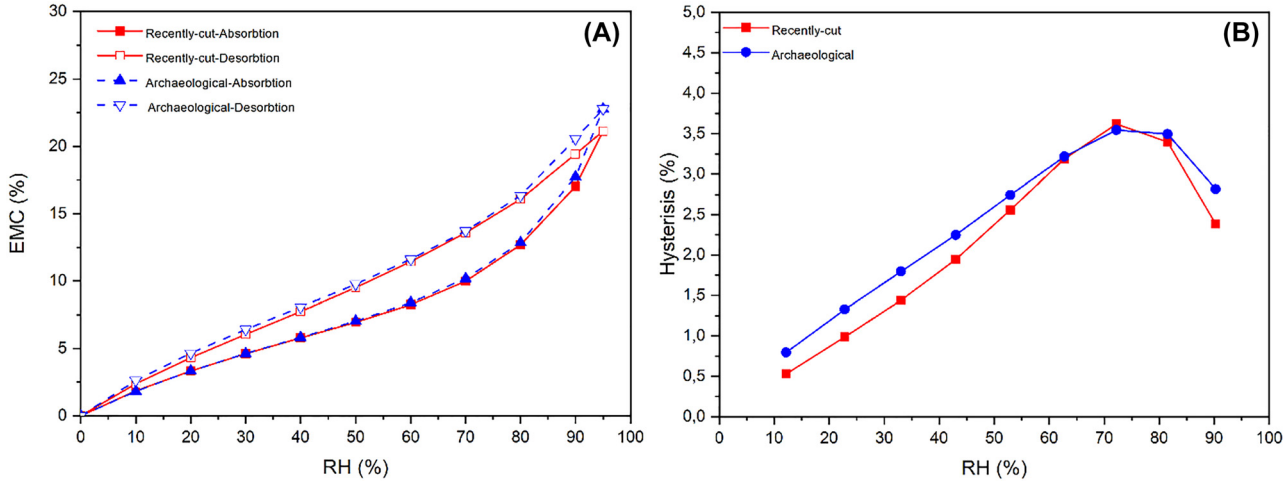

Figure 4: Adsorption and desorption isotherms (A) and sorption hysteresis (B) of recently-cut and archaeological oak at changing RH levels.

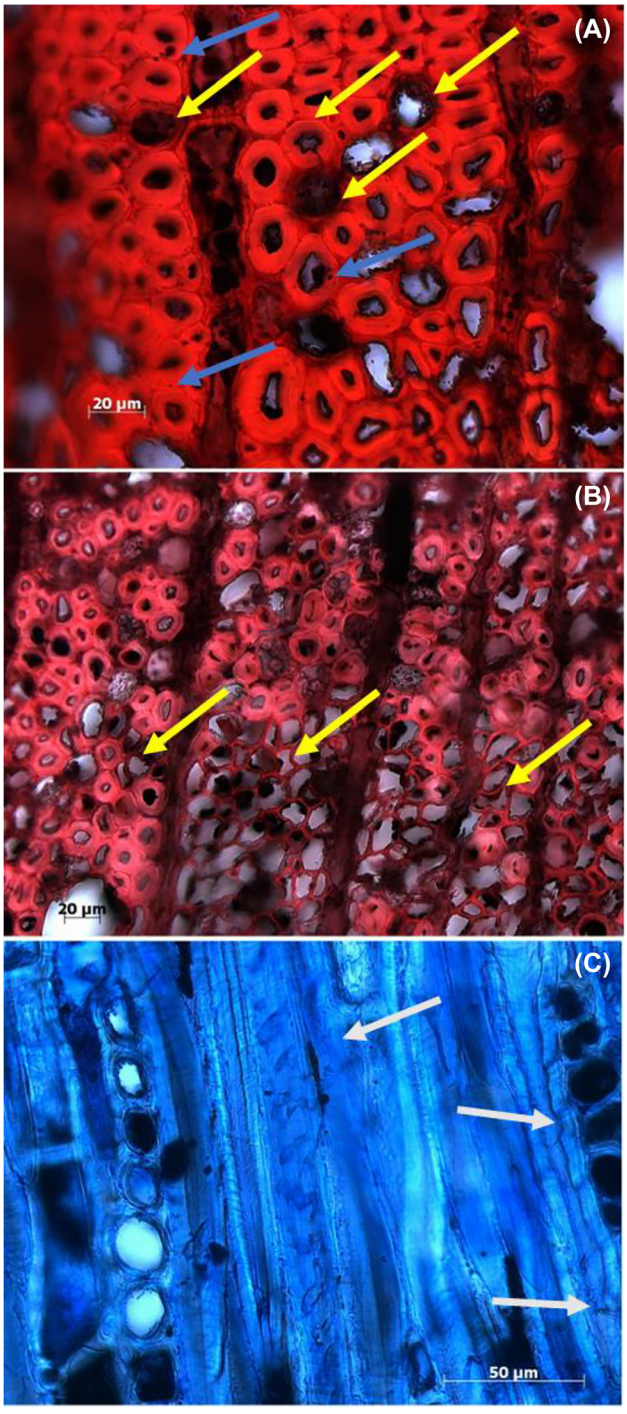

Figure 5: Light microscopic images of transverse sections of archaeological oak (A, B) showing cell wall erosion (arrows) and a tangential section using polarised light showing cell wall damage (C).

where the damage stopped. Lignin levels are typically highest in the primary cell wall and middle lamella, but this region is not directly affected by the bacterial attack. Lignin is present at proportionally lower levels in the secondary cell walls, but its presence appears to reduce cellulose degradation. In addition, lignin creates a physical barrier that affects and reduces the biological degradation of cellulose (Singh et al. 2022). This pattern again supports the premise that bacterial decay largely affected the carbohydrates such as cellulose and hemicellulose, leaving a lignin-rich fraction. This attack pattern is consistent with an attack by erosion bacteria (EB) as previously described (Cha et al. 2021; Nilsson and Björdal 2008; Singh et al. 2022). A similar pattern was also observed in the longitudinal sections as the characteristic fine ducts could be found in the longitudinal section (Figure 5C, arrows). No fungal hyphae were detected in the transverse or tangential sections.

The scanning electron (SEM) micrographs of archaeological oak showed no evidence of extensive damage to the rays, vessels, or fibers (Figure 6). Even the tyloses were intact in the vessels (yellow arrow in Figure 6C). Since the archaeological oak was underground for over 600 years, there was evidence of soil infusion into the wood cells, especially in the parenchyma, which is consistent with prolonged timber burial (Huisman et al. 2008; Smith and Lillie 2007). No evidence of fungal activity was found in SEM images. Partial cell wall degradation was infrequent, suggesting that bacterial degradation was still at a relatively early stage (green arrow in Figure 6B). The absence of fungal hyphae does not completely eliminate them as possible degradation agents but the absence of any hyphae suggests that they were not primary agents under these conditions.

The rod-shaped erosion bacteria were observed using field emission SEM (FESEM) (Figure 6E, F). These bacteria often had pointed ends and were 102 µm long, which was consistent with previous reports (Daniel 2014). Nilsson and Björdal (2008) found that erosion bacteria required special conditions for isolation and were only active under limited-oxygen conditions. The degradation patterns of EB are comparable to the soft-rot, where the bacteria align with the underlying cellulose microfibrils in the cellulose-rich S_2 cell wall layer. The location of EB in this cell wall zone may help explain how they primarily degrade cellulose (Daniel 2014; Nilsson and Björdal 2008; Singh et al. 2022).

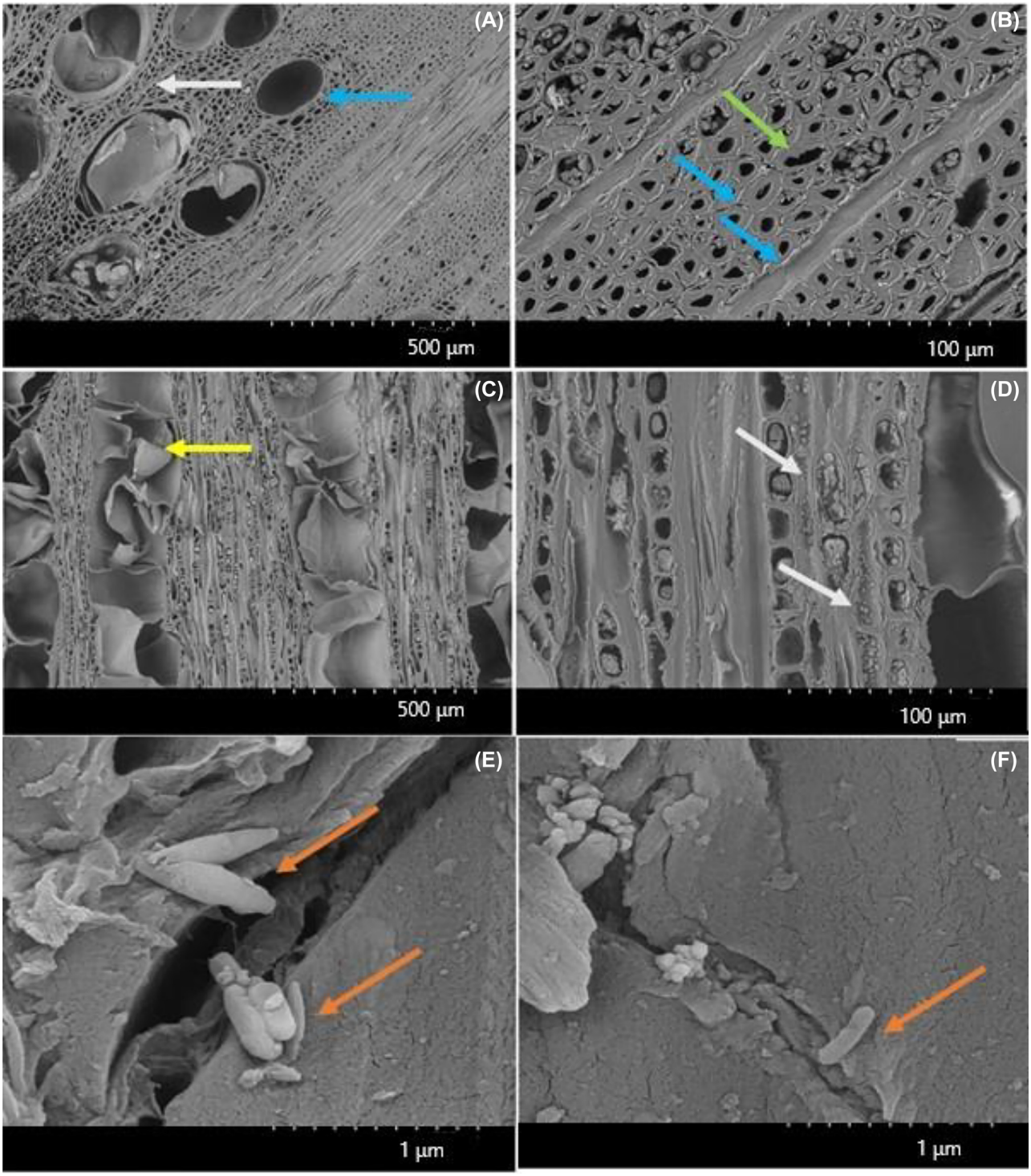

Figure 6: Scanning electron (SEM) micrographs of transverse (A, B), and tangential sections (C, D) of archaeological oak showing bacteria, cell wall erosion, and collapsed ray cells (Arrows). Field emission scanning electron microscograph (FESEM) (E, F) of archaeological oak wood showing erosion bacteria (orange arrows) on the wood cell wall.

4 Conclusions

Understanding the wood degradation state and mechanism is important for predicting the durability of structures and protecting existing monuments. The archaeological oak collected in this study from oxygen-limited conditions illustrated that its chemical composition, crystalline structure, and sorption behavior were very similar to those of recently-cut samples. Although the archaeological and recently-cut wood samples were nearly identical in the macro-observations, micro-structural analyses through optical and electron microscopy revealed that the degradation in the archaeological wood mainly occurred by erosion bacteria, which are active under oxygen-limited conditions. This study increased our knowledge of the importance of quality assessment in archaeological monuments, where decisions must be made to select proper protection and preservation methods for extending the lifespan of wooden buildings.

Author contributions: AG, RH and IS designed the research project; AG, MB, AJ, JG and JM mainly conducted experiments and wrote the manuscript; RH and IS supervised the work. All authors contributed to and approved the final version of the manuscript.

Research funding: None declared.

Conflict of interest statement: The authors declare that they have no known competing financial interests or personal relationships that could have appeared to influence the work reported in this paper.

Data availability: Data will be made available on request.

References

Baar, J., Paschová, Z., Hofmann, T., Kolář, T., Koch, G., Saake, B., and Rademacher, P. (2020). Natural durability of subfossil oak: wood chemical composition changes through the ages. Holzforschung 74: 47–59.

Björdal, C.G., Daniel, G., and Nilsson, T. (2000). Depth of burial, an important factor in controlling bacterial decay of waterlogged archaeological poles. Int. Biodeterior. Biodegrad. 45: 15–26.

Bjurhager, I., Halonen, H., Lindfors, E.L., Iversen, T., Almkvist, G., Gamstedt, E.K., and Berglund, L.A. (2012). State of degradation in archeological oak from the 17th century Vasa ship: substantial strength loss correlates with reduction in (holo)cellulose molecular weight. Biomacromolecules 13: 2521–2527.

Capano, M., Pignatelli, O., Capretti, C., Lazzeri, S., Pizzo, B., Marzaioli, F., Martinelli, N., Gennarelli, I., Gigli, S., Terrasi, F., et al. (2015). Anatomical and chemical analyses on wooden artifacts from a Samnite sanctuary in Hirpinia (Southern Italy). J. Archaeol. Sci. 57: 370–379.

Cha, M.Y., Lee, K.H., Kim, J.S., and Kim, Y.S. (2021). Variations in bacterial decay between cell types and between cell wall regions in waterlogged archaeological wood excavated in the intertidal zone. IAWA J. 42: 457–474.

Christiernin, M., Notley, S.M., Zhang, L., Nilsson, T., and Henriksson, G. (2009). Comparison between 10,000-year old and contemporary spruce lignin. Wood Sci. Technol. 43: 23–41.

Daniel, G. (2014). Fungal and bacterial biodegradation: white rots, brown rots, soft rots, and bacteria. In: *ACS symposium series*, pp. 23–58.

Dao, T.T., Gentsch, N., Mikutta, R., Sauheitl, L., Shibistova, O., Wild, B., Schnecker, J., Bárta, J., Čapek, P., Gittel, A., et al. (2018). Fate of carbohydrates and lignin in north-east Siberian permafrost soils. Soil Biol. Biochem. 116: 311–322.

Esteban, L.G., de Palacios, P., García Fernández, F., Martín, J.A., Génova, M., and Fernández-Golfín, J.I. (2009). Sorption and thermodynamic properties of buried juvenile Pinus sylvestris L. wood aged 1,170 ± 40 BP. Wood Sci. Technol. 43: 679–690.

Feist, W.C. (1989). Outdoor wood weathering and protection. In: *Archaeological wood, advances in chemistry*, 225. American Chemical Society, Washington, D.C., USA, pp. 263–298.

Florian, M.L.E. (1989). Scope and history of archaeological wood. In: *Archaeological wood, advances in chemistry*, 225. American Chemical Society, Washington, D.C., USA, pp. 3–32.

Gelbrich, J. (2009). Bacterial wood degradation: a study of chemical changes in wood and growth conditions of bacteria. In: *Secondary xylem biology*. Sierke Verlag, Gottingen, Germany, pp. 169–190.

Gelbrich, J., Mai, C., and Militz, H. (2008). Chemical changes in wood degraded by bacteria. Int. Biodeterior. Biodegrad. 61: 24–32.

Ghavidel, A., Hosseinpourpia, R., Militz, H., Vasilache, V., and Sandu, I. (2020a). Characterization of archaeological European white elm (Ulmus laevis P.) and black poplar (Populus nigra L.). Forests 11: 1329.

Ghavidel, A., Scheglov, A., Karius, V., Mai, C., Tarmian, A., Vioel, W., Vasilache, V., and Sandu, I. (2020b). In-depth studies on the modifying effects of natural ageing on the chemical structure of European spruce (Picea abies) and silver fir (Abies alba) woods. J. Wood Sci. 66: 77.

Ghavidel, A., Gelbrich, J., Kuqo, A., Vasilache, V., and Sandu, I. (2020c). Investigation of archaeological European white elm (Ulmus laevis) for identifying and characterizing the kind of biological degradation. Heritage 3: 1083–1093.

Ghavidel, A., Hofmann, T., Bak, M., Sandu, I., and Vasilache, V. (2020d). Comparative archaeometric characterisation of recent and historical oak (Quercus spp.) wood. Wood Sci. Technol. 54: 1121–1137.

Ghavidel, A., Bak, M., Hofmann, T., Vasilache, V., and Sandu, I. (2021a). Evaluation of some wood-water relations and chemometric characteristics of recent oak and archaeological oak wood (Quercus robur) with archaeometric value. J. Cult. Herit. 51: 21–28.

Ghavidel, A., Hosseinpourpia, R., Gelbrich, J., Bak, M., and Sandu, I. (2021b). Microstructural and chemical characteristics of archaeological white elm (ulmus laevis P.) and poplar (populus spp.). Appl. Sci. 11: 10271.

Ghavidel, A., Bak, M., Hofmann, T., Hosseinpourpia, R., Vasilache, V., and Sandu, I. (2022). Comparison of chemical compositions in wood and bark of persian silk tree (*Albizia julibrissin* Durazz.). Wood Mater. Sci. Eng. 17: 759–770.

Goodell, B., Winandy, J.E., and Morrell, J.J. (2020). Fungal degradation of wood: emerging data, new insights and changing perceptions. Coatings 10: 1210.

Guo, J., Zhou, H., Stevanic, J.S., Dong, M., Yu, M., Salmén, L., and Yin, Y. (2018). Effects of ageing on the cell wall and its hygroscopicity of wood in ancient timber construction. Wood Sci. Technol. 52: 131–147.

Han, L., Guo, J., Wang, K., Grönquist, P., Li, R., Tian, X., and Yin, Y. (2020). Hygroscopicity of waterlogged archaeological wood from Xiaobaijiao no.1 shipwreck related to its deterioration state. Polymers 12: 834.

Howell, C., Hastrup, A.C.S., Goodell, B., and Jellison, J. (2009). Temporal changes in wood crystalline cellulose during degradation by brown rot fungi. Int. Biodeterior. Biodegrad. 63: 414–419.

Hedges, J.I. (1989). The chemistry of archaeological wood. In: *Archaeological wood properties, chemistry, and preservation (Chapter 5)*. American Chemical Society, Washington, D.C., USA, pp. 111–140.

Hosseinpourpia, R., Adamopoulos, S., and Mai, C. (2016). Dynamic vapour sorption of wood and holocellulose modified with thermosetting resins. Wood Sci. Technol. 50: 165–178.

Hosseinpourpia, R., Adamopoulos, S., and Mai, C. (2018). Effects of acid pre-treatments on the swelling and vapor sorption of thermally modified Scots pine (Pinus sylvestris L.) Wood. Bioresources 13: 331–345.

Hosseinpourpia, R., Adamopoulos, S., and Parsland, C. (2019). Utilisation of different tall oils for improving the water resistance of cellulosic fibers. J. Appl. Polym. Sci. 136: 47303.

Hosseinpourpia, R., Adamopoulos, S., Walther, T., and Naydenov, V. (2020). Hydrophobic formulations based on tall oil distillation products for high-density fiberboards. Materials 13: 4025.

Huisman, D.J., Manders, M.R., Kretschmar, E.I., Klaassen, R.K.W.M., and Lamersdorf, N. (2008). Burial conditions and wood degradation at archaeological sites in The Netherlands. Int. Biodeterior. Biodegrad. 61: 33–44.

Jingran, G., Jian, L., Jian, Q., and Menglin, G. (2014). Degradation assessment of waterlogged wood at Haimenkou site. Frat. Ed. Integrità Strutt. 30: 495–501.

Kránitz, K., Sonderegger, W., Bues, C.T., and Niemz, P. (2016). Effects of aging on wood: a literature review. Wood Sci. Technol. 50: 7–22.

Lionetto, F., Sole, R.D., Cannoletta, D., Vasapollo, G., and Maffezzoli, A. (2012). Monitoring wood degradation during weathering by cellulose crystallinity. Materials 5: 1910–1922.

Lucejko, J.J., Tamburini, D., Zborowska, M., Babiński, L., Modugno, F., and Colombini, M.P. (2020). Oak wood degradation processes induced by the burial environment in the archaeological site of Biskupin (Poland). Heritage Science 8: 44.

Łojewska, J., Miśkowiec, P., Łojewski, T., and Proniewicz, L.M. (2005). Cellulose oxidative and hydrolytic degradation: in situ FTIR approach. Polym. Degrad. Stabil. 88: 512–520.

Nilsson, T. and Björdal, C. (2008). Culturing wood-degrading erosion bacteria. Int. Biodeterior. Biodegrad. 61: 3–10.

Nzokou, P. and Pascal Kamdem, D. (2005). X-ray photoelectron spectroscopy study of red oak-(Quercus rubra), black cherry-(Prunus serotina) and red pine-(Pinus resinosa) extracted wood surfaces. Surf. Interface Anal. 37: 689–694.

Pedersen, N.B., Łucejko, J.J., Modugno, F., and Björdal, C. (2021). Correlation between bacterial decay and chemical changes in waterlogged archaeological wood analysed by light microscopy and Py-GC/MS. Holzforschung 75: 635–645.

Popescu, C-M. and Hill, C.A.S. (2013). The water vapour adsorption–desorption behaviour of naturally aged Tilia cordata Mill. wood. Polym. Degrad. Stabil. 98: 1804–1813.

Popescu, C-M., Tibirna, C-M., and Vasile, C. (2009). XPS characterisation of naturally aged wood. Appl. Surf. Sci. 256: 1355–1360.

Singh, A.P., Kim, Y.S., and Chavan, R.R. (2022). Advances in understanding microbial deterioration of buried and waterlogged archaeological woods: a review. Forests 13: 394.

Smith, R. and Lillie, M. (2007). Using a lysimeter study to assess the parameters responsible for oak wood decay from waterlogged burial environments and their implication for the in situ preservation of archaeological remains. Int. Biodeterior. Biodegrad. 60: 40–49.

Unger, A., Schniewind, A., and Unger, W. (2001). *Conservation of wood artifacts: a handbook*. Springer Science & Business Media, Berlin, Germany.

Walsh-Korb, Z. and Avérous, L. (2019). Recent developments in the conservation of materials properties of historical wood. Prog. Mater. Sci. 102: 167–221.